Lab on a Chip

Cite this: *Lab Chip*, 2012, **12**, 3566–3575

www.rsc.org/loc

CRITICAL REVIEW

Optical imaging techniques in microfluidics and their applications†

Jigang Wu,*[a] Guoan Zheng[b] and Lap Man Lee[c]

Received 6th May 2012, Accepted 28th June 2012
DOI: 10.1039/c2lc40517b

Microfluidic devices have undergone rapid development in recent years and provide a lab-on-a-chip solution for many biomedical and chemical applications. Optical imaging techniques are essential in microfluidics for observing and extracting information from biological or chemical samples. Traditionally, imaging in microfluidics is achieved by bench-top conventional microscopes or other bulky imaging systems. More recently, many novel compact microscopic techniques have been developed to provide a low-cost and portable solution. In this review, we provide an overview of optical imaging techniques used in microfluidics followed with their applications. We first discuss bulky imaging systems including microscopes and interferometer-based techniques, then we focus on compact imaging systems that can be better integrated with microfluidic devices, including digital in-line holography and scanning-based imaging techniques. The applications in biomedicine or chemistry are also discussed along with the specific imaging techniques.

Introduction

Microfluidics[1,2] is an emerging area that has attracted significant research effort in the fields of biology, medicine, and chemistry. Microfluidic devices rely on micron-scale structures to handle samples, such as reaction agents, cells, *etc.* Because of the small size—usually ranging from tens to hundreds of microns—of microfluidic channels, microfluidic technology has the advantages of consuming fewer samples and having faster reaction rates for analytic processes. Optofluidics[3–5] is the fusion of optics and microfluidics that applies optical technologies in the microfluidic devices. Since the invention of the word "optofluidics" in around 2003, it has become an increasingly active area.[6]

Within the area of optofluidics, optical detection is important for extracting information from microfluidic devices. Review articles for optical detection methods, such as those based on refractive index measurement, absorbance, fluorescence, and Raman spectroscopy, are available in the literature.[7–11] Recently, there has been growing research interest in optical imaging techniques, especially compact or on-chip imaging methods, which can provide a microscopic image of samples in microfluidic channel that usually contains more information than

[a]*Biophotonics Laboratory, University of Michigan–Shanghai Jiao Tong University Joint Institute, Shanghai Jiao Tong University, Shanghai, 200240, China. E-mail: jigang.wu@sjtu.edu.cn*
[b]*Department of Electrical Engineering, California Institute of Technology, Pasadena, CA, 91125, USA. E-mail: gazheng@caltech.edu*
[c]*Department of Bioengineering, California Institute of Technology, Pasadena, CA, 91125, USA. E-mail: lmlee@caltech.edu*
† Published as part of a themed issue on optofluidics

Jigang Wu

Dr Jigang Wu is an assistant professor at the University of Michigan-Shanghai Jiao Tong University (UM-SJTU) Joint Institute, Shanghai, China. He received his B.S. and M.S. in Physics from Tsinghua University in 2001 and 2004, respectively, and Ph.D. in Electrical Engineering from the California Institute of Technology in 2008. His research interests include biomedical optical imaging and biophotonics with emphasis on developing novel imaging methods and seeking applications in biomedical research and clinical diagnosis.

Guoan Zheng

Guoan Zheng received a B.S. degree with Honors in Electrical Engineering from Zhejiang University, China, in 2007, his M.S. and Ph.D. degrees in 2008 and 2012 (expected) from California Institute of Technology, all in Electrical Engineering. He is the recipient of the Lemelson-MIT Caltech student prize for his contributions on chip-scale microscopy imaging.

other detection methods. In this review, we will deliver a survey on optical imaging methods that can be applied to detection in microfluidic devices. We will also discuss the potential applications of these imaging methods.

In many applications, optical imaging techniques, especially microscopic imaging techniques are required to observe the samples in microfluidic channels. Interferometer based imaging techniques, such as optical coherence tomography, are also used in some circumstances. On the one hand, conventional microscopes and other bulky optical imaging techniques are commonly used for observing microfluidic devices. In these situations, microfluidic devices can be directly put into the imaging systems, which are usually well developed. However, the bulky nature of conventional microscopes and similar imaging systems is not aligned well with the compact on-chip microfluidic devices. On the other hand, significant research efforts have also been devoted to develop compact imaging systems that can be readily integrated with microfluidics devices. The compact imaging systems can be divided into two different categories. In one category, the imaging systems are generally developed based on conventional lens imaging. They are specially designed to be compatible with the on-chip microfluidic devices. In the other category, lensless imaging systems are developed to get rid of the lens in order to make more compact on-chip systems. Examples of these imaging techniques include direct shadow imaging, digital in-line holography, and scanning-based technologies such as optofluidic microscopy. The review paper by Gurkan *et al.*[12] and Zheng[13] discussed some of the lensless imaging systems for point-of-care testing and chip-scale imaging systems that can also be used in microfluidic devices.

Optical imaging techniques in microfluidics can be divided into fluorescent and non-fluorescent methods. Fluorescence imaging is very useful to observe cells or organelles that can be tagged with fluorophores. However, fluorescence imaging systems are usually more complicated than non-fluorescence ones. For bulky optical imaging techniques used in microfluidics, such as the conventional microscope, achieving fluorescence imaging is quite simple. But for some compact or on-chip imaging techniques, fluorescence imaging is not easy. We will discuss the fluorescence capability of various optical imaging systems in later sections.

Lap Man Lee

Dr Lap Man Lee graduated (with first-class Honors) from the Department of Mechanical Engineering, the Hong Kong University of Science and Technology, in 2003. He received his M.Sc. degree in aerospace and mechanical engineering at the University of Arizona, Tucson, in 2006. Then, he moved to the California Institute of Technology, Pasadena and obtained his Ph.D. degree in Bioengineering, in 2012. His research interests include optofluidics, biomedical microdevices, lab-on-a-chip, microfluidics and electrokinetics.

It is worth noting that the research on optical imaging in microfluidics does not limit itself to the optics part. Researchers have also worked on the microfluidics part to facilitate optical imaging, especially for fluorescence imaging. This can be achieved by fabricating special structures, such as plasmonic nanostructures,[14] zero-mode waveguides,[15] and sub-wavelength slot waveguides[16] to enhance the signal. Surface passivation strategies can also be used to reduce the noise, such as applying bovine albumin (BSA)[17] or poly(ethylene glycol) (PEG)[17,18] on the surface. The review paper by Vasdekis *et al.*[19] is devoted to discussion of these techniques to enhance single molecule imaging, and we are not going to cover the details of these research efforts.

The structure of this review is arranged as follows: in the next section, we will briefly overview the bulky optical imaging techniques used in microfluidics. We then discuss the digital in-line holography techniques, which can be achieved without using conventional lens. This is followed by the discussion of scanning-based imaging techniques, where images are acquired by scanning of the sample or the illumination light. Before concluding this review, we present other compact imaging systems that can be well integrated with the on-chip microfluidic device.

Bulky optical imaging techniques

Conventional microscopes have been used to observe microfluidic devices since the early development of microfluidics. The advantage of using conventional microscopy techniques is that the imaging systems are well developed and commercial products are available. In this case, the imaging system and the microfluidic device are not integrated and usually independent of each other. Various microscope techniques have been applied in microfluidics, including bright-field and fluorescence microscopy,[20–24] phase contrast microscopy,[25] differential interference contrast (DIC) microscopy,[26] laser scanning confocal microscopy,[27] and single-molecule imaging techniques[28–31] *etc.* Note that in some cases, especially for fluorescence and single-molecule detection, microfluidic devices can be specially designed to enhance the signal to noise ratio (SNR) as discussed earlier. Since conventional microscopy is well-developed, the details won't be discussed in this review.

Besides conventional microscopy, interferometer based imaging techniques are also used in microfluidics. One important example is optical coherence tomography (OCT).[32] OCT is based on low-coherence interferometery and has been developed as a powerful imaging modality for biomedical imaging.[33] The axial resolution of OCT is normally around 10 microns and worse than normal microscopy. So usually OCT is not used to obtain images of the samples in the microfluidic channel. Instead, it can be used to measure the flow velocity of the fluid in microfluidic channels[34–39] in the form of optical Doppler tomography (ODT) or Doppler OCT. With Doppler OCT, the cross-section flow speed in the microfluidic channel can be measured directly, which is usually not straightforward for other imaging techniques. OCT can be divided into time-domain[34–37] and spectral-domain systems,[38,39] and currently the latter is predominantly used because of its advantages in terms of signal-to-noise ratio (SNR) and imaging speed.[40]

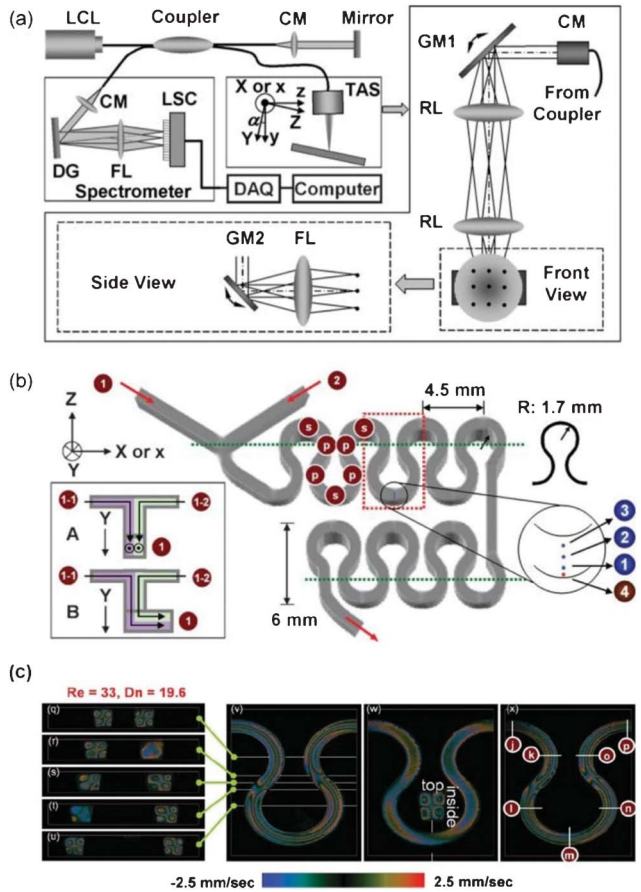

Fig. 1 (a) A typical setup for Doppler OCT system; (b) a meandering square microchannel for observing fluidic mixing; (c) the liquid velocity measurement. Images are acquired from ref. 38.

A typical setup for a Doppler OCT system[38] is shown in Fig. 1(a), where the spectral domain OCT is used. It is worth noting that Doppler OCT can measure the speed only when its direction is not perpendicular to the optic axis. Otherwise there will be no Doppler shift. The phase of the interference fringes in OCT will change with the fluid flow velocity in the microfluidic channel because of the Doppler effect. The flow velocity can thus be calculated according to this phase change. When the microfluidic channel is perpendicular to the optic axis, the detected velocity will not include the primary flow. In this case, secondary flow velocities can be characterized precisely. Note that in Fig. 1(a), the fluid channel was deliberately tilted at a small angle with respect to the optical axis in order to reduce the strong back scattering from the top and bottom surfaces. Ahn *et al.*[38] use the spectral- domain Doppler OCT system to observe secondary flow and mixing in a meandering microchannel. Fig. 1(b) shows the microchannel and Fig. 1(c) shows an example of their measurement.

Besides intensity images of microfluidic devices, phase changes can be observed by interferometer-based phase imaging methods.[41,42] The phase changes are usually caused by refractive index change of the sample or fluid in the microfluidic channel. Compared with fluorescence or other nonlinear imaging techniques for enhancing image contrast, phase imaging has the advantage of being a label-free method, and thus special preparation of the sample is not necessary. Conventional phase imaging technologies are generally qualitative, such as phase contrast and DIC microscopy. More recently, various quantitative phase imaging techniques have been developed.[41] In the case of observing microfluidic devices, the phase change of the sample can be measured quantitatively and can be converted into the change of refractive index given the thickness of the microfluidic channel. For example, Lue *et al.* used Hilbert phase microscopy to observe HeLa cells in microchannels,[42] as shown in Fig. 2. Here the microchannel acted to confine the live cell so as to separate the contributions to phase signal from the cell refractive index and thickness. Another example of the application of phase imaging techniques is to observe the mixing of different fluids in microchannels, which is important in many situations and often observed by adding dyes into the fluids and then observing the changes in color.[43] In this case, phase imaging provides an alternative solution. Wu *et al.* used a phase imaging method to observe the refractive index change in microfluidic channels,[44] as shown in Fig. 3. It can be seen that the mixing of two types of fluids, here water and saltwater, with different refractive indices can then be easily observed by the phase imaging methods.

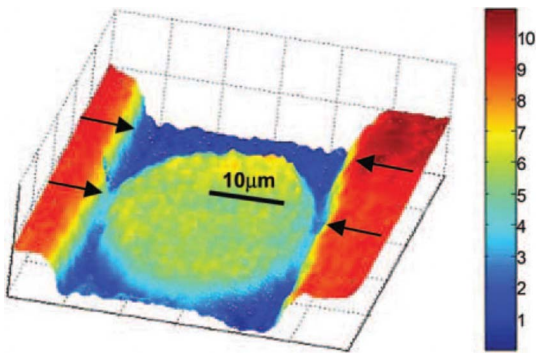

Fig. 2 Quantitative phase image of a HeLa cell in a microchannel (color bar indicates phase in radians). Image is acquired from ref. 42.

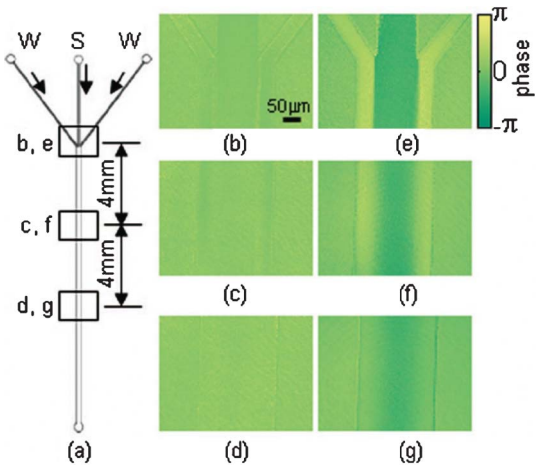

Fig. 3 Observation of microfluidic mixing and diffusion process of water (W) and saltwater (S) by quantitative phase imaging. Images are acquired from ref. 44.

Besides measuring phase by interferometer, intensity images can be used to compute phase image by using the transport-of-intensity-equation method.[45] Gorthi *et al.* described a good example of combining microfluidics and intensity imaging to achieve phase image flow cytometry using a focus-stack collecting microscope.[46] As shown in Fig. 4, the microfluidic device is tilted at an angle with respect to the optical axis. This allowed acquisition of sample images at different focal positions as the sample is flowing through the microchannel. These images can then be used to compute quantitative phase image of the sample.

Like the flow speed, measuring pressure in microfluidic channels is important for many applications.[47–49] Pressure in a microchannel is usually measured with external pressure transducers and it's difficult to measure the local pressure accurately. Song *et al.* introduced the technique of an optofluidic membrane interferometer that can measure the microfluidic pressure and flow rate simultaneously.[50] In their setup, an air-gap cavity is built on top of a microfluidic channel, with a polydimethylsiloxane (PDMS) membrane in between. The height of the air cavity will be changed as the PDMS membrane is deformed by the pressure in the microfluidic channel. Under the illumination of monochromatic light, reflection from the top and bottom of the air cavity will interfere and generate fringes, which change with the cavity height. The fringe changes can then be used to determine the PDMS membrane deformation and thus the pressure.

Currently, conventional microscopy and other bulky imaging techniques are still prevailing in the research and application of microfluidics. And they provide the most versatile imaging modalities to be used in microfluidics.

Digital in-line holography

In-line holography represents a lensless microscopy approach invented by Gabor[51] in 1948. In Gabor's original setup, the sample is placed between a coherent light source and a photographic plate. The light incident on the sample will be scattered and interfere with the undisturbed light. The imaging process involves two steps: 1) record the interference pattern on the photographic plate, *i.e.*, the hologram, and 2) reconstruct the object image with another light source. The advantage of using holographic method is that the intensity and phase information of the sample can be recorded and then reconstructed simultaneously. However the use of another light source for reconstruction prevents real-time imaging, and thus makes this approach impractical for a lot of applications. So it has received only limited attentions in the area of microscopic imaging since its debut in 1940s.

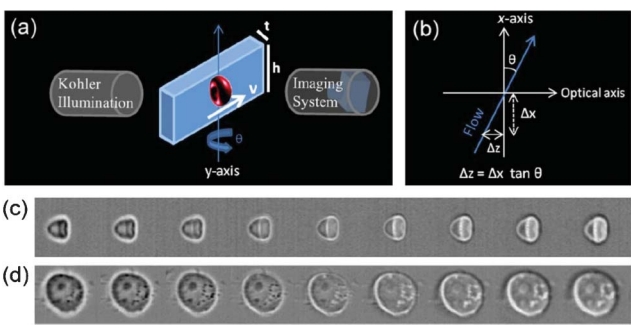

Fig. 4 (a) Schematic of the focus-stack collecting microscope; (b) top view of the schematic; (c), (d) focus stacks of an individual red blood cell and a leukemia cell. Images are acquired from ref. 46.

In recent years, the development of digital imaging sensors has significantly improved and simplified the procedure of in-line holography. The image reconstruction step of in-line holography can be effectively performed numerically using a personal computer. As such, the combination of in-line setup with digital recording devices and numerical reconstruction processes, termed digital in-line holography (DILH), has regained much popularity in the last couple of years.[52–57] Due to the simplicity of DILH setup, it can also be seamlessly integrated with microfluidic devices, and thus, enables new opportunities in the context of optofluidics.

The typical scheme of DILH is shown in Fig. 5, where the light source is placed in front of a pinhole and the sample (a microfluidic channel) is placed on top of a CCD/CMOS image sensor. The use of pinhole increases the spatial coherence length of the light. The electric-field from the pinhole is called the reference field, denoted as $E_{ref}(x,z)$. Such a reference field is incident upon the sample with amplitude transmittance $t(x)$. We note that $t(x)$ is a complex-valued function; its magnitude indicates the light absorption of the object and its phase indicates the optical path length change induced by the object. The resulting electric-field at the sample plane is

$$E_{ref}(x,z_0)t(x) \approx E_{ref}(x)(1 + \Delta t(x)) = E_{ref}(x,z_0) + E_{sca}(x,z_0) \quad (1)$$

Where E_{sca} is the scattering electric-field induced by the sample. There is an approximation of the sample transmittance in eqn (1), *i.e.*, $t(x) \approx 1 + \Delta t(x)$. This approximation is based on first-order Taylor expansion and it is only valid for weakly

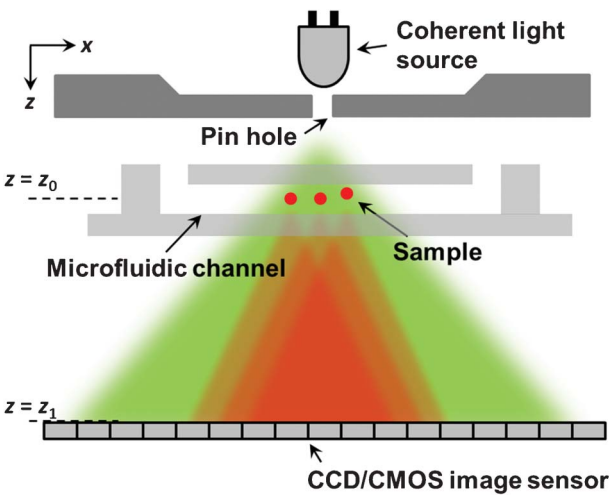

Fig. 5 The typical setup of digital in-line holographic microscope for microfluidic applications. The light source is spatially filtered by a pinhole for increasing the coherence length. The sample (a microfluidic device) is placed between the light source and the image recording plane. The scattering wave from the sample interferes with the reference wave from the light source and forms a hologram for digital recording.

scattering objects. Under this approximation, the intensity at the imaging sensor, *i.e.*, the hologram, can be expressed as

$$I = |E_{\mathrm{ref}}(x,z_1) + E_{sca}(x,z_1)|^2 = |E_{\mathrm{ref}}(x,z_1)|^2 + |E_{\mathrm{sca}}(x,z_1)|^2 + E_{\mathrm{ref}}^{*}(x,z_1)E_{\mathrm{sca}}(x,z_1) + E_{\mathrm{ref}}(x,z_1)E_{\mathrm{sca}}^{*}(x,z_1) \quad (2)$$

where the last two terms correspond to the real and the twin image, respectively. There are two strategies to reconstruct the image of the sample. The first approach is to recover $E_{\mathrm{sca}}(x,z_1)$ in eqn (2). This is the digital version of the traditional holographic reconstruction method[58,59] and can be achieved by multiplying the reference field to the hologram and propagate the field at the distance $z_1 - z_0$. The algorithm is straight-forward. However, the real and twin images cannot not be separated in this case. And the approach is valid only when the sample is weekly scattering. The second approach is to recover $E_{\mathrm{ref}}(x,z_0)t(x)$ in eqn (1) directly and thus free of the twin-image problem. This can be achieved by the iteration methods developed by Fienup *et al.*[60,61] and other researchers.[62–64] The typical image recovery process involves light field propagation back and forth between the imaging domain $z = z_1$ (where the intensity data are applied) and object domain $z = z_0$ (where *a priori* object constrains are applied). Other reconstruction methods have also been developed to remove the twin-image artifact.[65–67]

The combination of DILH platform and microfluidic devices holds great potentials for different applications. Garcia-Sucerquia *et al.* first demonstrated the application of DILH for a microfluidic platform.[68] They recorded the three dimensional trajectories of microspheres and red blood cells inside a microfluidic channel, with a micron-level spatial resolution and a sub-second level temporal resolution. Applications of such a platform include studies of colloidal suspensions, investigation of bacterial attachment and particle velocimetry.

The early development of DILH is based on the use of a laser source, which provides supreme spatial and temporal coherence. However, imaging performance is greatly limited by coherent-based noises, such as speckles and cross-interferences. Repetto *et al.* first employed a partially coherent light source (LED) for the DILH platform.[52] The elimination of speckle noise and the reduction of cost by using a partially coherent light source enable new opportunities in resource-limited applications. Along this line, Bishara *et al.* integrated the LED-based DILH platform with a microfluidic channel for sample transporting, termed holographic optofluidic microscopy (HOM).[69] In this platform, a microfluidic channel was placed on top of a CMOS image sensor. An LED was used as a light source and a 0.1 mm aperture was used as spatial filter to increase the coherence length. Light scattered by the sample interfered with the reference light to form a hologram on the CMOS pixel array. A single recorded hologram can be used to recover the image of the sample, with a resolution limit imposed by the pixel size. To circumvent this limitation, multiple holograms, which are subpixel-shifted with respect to each other, can be combined to achieve a higher resolution hologram. This high-resolution hologram can then be used to recover the image of the object, with a demonstrated micron-level resolution. Fig. 6 shows their imaging results for a *Giardia lumblia* cyst and a mulberry pollen sample flowing through the microfluidic channel. This technique has the potential to advance the capabilities of optofluidic

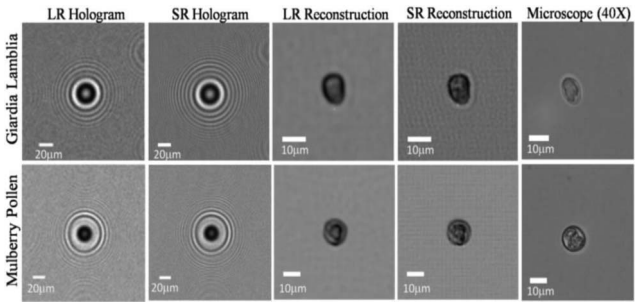

Fig. 6 HOM imaging results for a *Giardia lamblia* cyst and a mulberry pollen particle. LR: low-resolution, SR: super-resolved. Images are acquired from Ref. 69.

imaging and analysis by performing rapid cell counting and phenotyping.

Despite the simplicity and cost-effectiveness of the DILH approach, there are also several limitations worth discussing. First, the image recovery process relies on the imposed object support of the sample. Generally speaking, it only works well for the samples that are spatially sparse.[61,70,71] Second, due to the stagnation problem,[72] the solution is not guaranteed in the iterative phase recovery process. To address these issues, off-line holography approaches with various phase extracting techniques, where the reference wave is separately introduced to the image recording plane, has also been employed for microfluidic applications. Some of these approaches have been discussed in the previous section.[41,42] Another example is the optofluidic system with digital holographic microscopy developed by Shin *et al.*[73] At the cost of system complexity, they are capable of measuring both the intensity and the phase information separately and quantitatively. In contrast to DILH, object supports are not needed in these approaches, and as such, the image reconstruction process is deterministic and non-iterative.

Another disadvantage of DILH is the difficulty with fluorescence imaging, because of two reasons. First, the coherence of fluorescence light is generally not good enough for holography. Second, the illumination of the sample is not focused, thus the efficiency of fluorescence excitation is low compared to focused light illumination as in confocal microscope. Nevertheless, it is possible to a combine fluorescence imaging setup with DILH, as reported by Coskun *et al.*[74] However, the fluorescence image has limited resolution without the use of lenses.

Integrating microfluidic techniques in the DILH platform is still in its early stage. We envision two trends for further development. The first trend is the development of low-cost portable platforms. This is perhaps not unexpected, given the simplicity of the DILH setup. The second trend is the development of high throughput platforms, which requires full automation and sophisticated microfluidic techniques for sample handling.

Scanning-based imaging techniques

Two novel scanning-based optical imaging techniques have been developed and commercialized in the 20th century, resulting in ground-breaking discoveries in biology and biomedicine. The

first is confocal microscopy,[75] which was originally developed by Minsky in the 1950–60s.[76] Confocal microscopy is a far-field optical imaging method, uniquely characterized by a pinhole aperture and point-by-point illumination on the specimen. The pinhole rejects any out-of-focus light collected from the sample, leading to a reduction in background illumination light, increase in SNR and improvement in both lateral and axial resolution. The focused light illumination also helps to increase the fluorescence excitation efficiency. Different mechanical scanning strategies have been developed to direct the laser illumination spot to different parts of the biological specimen. Although several efforts have tried to miniaturize confocal microscopy systems by MEMS technology in the past decades,[77,78] the complicated mechanical actuation system is proving to be difficult and costly to miniaturize.

The second advancement is near-field scanning optical microscopy (NSOM/SNOM), which is able to break the far-field resolution limit. An illumination beam, which is diffraction limited, is coupled into a probe tip with a nano-aperture, which is smaller than one wavelength (for example, about 50 nm), and brought in closely to the sample surface. The nano-aperture probe creates a tightly localized light field in the form of an evanescent wave, interacting with scatterers on the sample surface. These near-field components are modified and converted into propagating far-field components so that they can be collected by collective optics and detected by a photodetector. The scanning feature of NSOM allows us to illuminate and detect a small area, defined by the resolution, of the sample at a time. Thus, the nano-aperture probe of a NSOM is able to differentiate nanoscale structures that are extremely close to each other with optical resolution of less than 100 nm.[79,80] The optical resolution of NSOM is fundamentally limited by the separation between the probe tip and sample which is usually within hundreds of nanometers and it requires an even more accurate and sophisticated mechanical feedback systems to ensure the probe is in close proximity with the sample surface throughout the scanning process. This is why it becomes technologically challenging to integrate NSOM systems at the chip level.

Two scanning optical imaging schemes have one characteristic in common: they require the actuation of illumination light spots to different parts of the sample while it is held steady. However, the scanning scheme needs not to be conducted this way. Instead, the illumination or collection optical configuration can be held steady while the specimen moves. This gives the opportunity for the microfluidics community to effectively miniaturize and simplify optical imaging at the chip scale level. Microfluidic flow is characterized by low Reynolds number. In this regime, fluid flow is dominated by viscous force. This tends to stabilize the microfluidic flow motion of biological specimens.

Optofluidic microscopy (OFM)[81] is a good example of microfluidic-based scanning optical microscope, where biological samples are delivered in a microfluidic channel and scanned by a linear array of sampling points. In 2006, the first proof of concept prototype OFM was developed.[81] A line of aperture array in a metal layer was fabricated on the floor of a PDMS microfluidic channel. The channel was tilted at certain angle so that the biological sample *C. elegans* could be translated on top of the aperture array under gravity. The light transmission through each aperture is relayed by a bulk microscope into

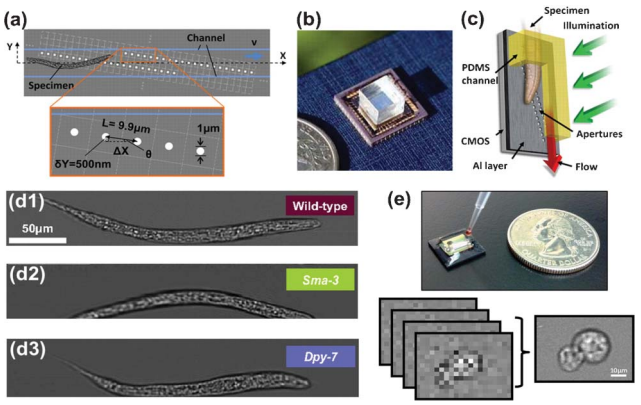

Fig. 7 OFM prototype. (a) Schematic of the device (top view). (b) The actual device compared with a U.S. quarter. (c) Upright operation mode. (d) Images of *C. elegans* acquired by OFM. (e) The subpixel resolving optofluidic microscope (SROFM). Images are acquired from ref. 82 and ref. 84.

individual pixels of a CCD imaging sensor. The best optical resolution obtained is about 500 nm. In 2008, OFM was implemented completely 'on-chip',[82] as shown in Fig. 7(a)–(c). The slanted line of apertures was fabricated directly on every alternate pixel of a CMOS imaging sensor using a focused ion beam (FIB). The OFM was used to image the nematode *C. elegans*, as shown in Fig. 7(d) . With better microfluidic control on the biological samples using DC electrokinetics, spherical/ellipsoidal biological samples, such as pollen spores, *Chlamydomonas*, and *Giardia lamblia* trophozoites and cysts, were able to be imaged at the high resolution of 800 nm.[82, 83]

Based on the first version of the aperture-based OFM device, a few derivatives of compact OFM devices have been developed over the following years. In 2010, a new version of the OFM device, termed the subpixel resolving OFM (SROFM) was been developed by Zheng *et al.*[84,85] This scheme eliminates the need for the metal mask and sub-micron apertures; instead, it employs the pixel super resolution algorithm to reconstruct a high-resolution image from a sequence of low-resolution images, as shown in Fig. 7(e). In a typical SROFM device, 40–50 raw images (limited by pixel size) are acquired as the sample flows across the channel. With a high-frame-rate imaging sensor, the total acquisition time can be much less than the aperture-based OFM. Because of this, the SROFM device is capable of imaging samples with different shapes flowing with non-uniform translational motion and even rotation under a low-speed pressure-driven flow condition.[84] Combined with color illumination, the SROFM device has also been demonstrated as a useful tool for identifying malaria infected red blood cells, with a resolution of 660 nm.[85]

Another variation of OFM is to use a Fresnel zone plate (FZP) fabricated on a glass plate to relay the light collected by the aperture to the imaging sensor.[86] The scheme is compact and can be used to separate the imaging sensor from the microfluidic device, and thus make it possible to recycle the imaging sensor after each use of the device and also enables the possibility of cooling the sensor to enhance sensitivity without affecting the sample because of the heat transfer isolation. Around the same time, the development of OFM has proceeded to another front

with using coherent light as the illumination source. A major effort has been carried out to integrate an array of FZPs on top of a microfluidic channel to generate an array of tightly focused light spots, with a resolution of 650 nm. This scheme has directly led to the development of the fluorescent OFM system,[87] in which, when a fluorescence biological sample flows through the channel and across the array of focused light spots, the fluorescent emissions are collected by a filter-coated CMOS sensor, which is coated on the floor of the microfluidic channel to render high resolution fluorescence images. For comparison, we notice that the fluorescence capability cannot be effectively implemented in the aperture based OFM scheme because of the fluorescence excitation and collection efficiency. A similar approach has been demonstrated by Schonbrun *et al.*,[88] where a 2-D array of phase reversal FZP was used to focus and collect light from fluorescent droplets in highly branched microfluidic channels for high-throughput imaging purposes. The light excitation and collection by the FZP microfluidic device in their setup is shown in Fig. 8.

Scanning-based optical imaging can also be conducted with focus line illumination. Heng *et al.* demonstrated a line-scan optofluidic imaging technique by using a precisely-defined line-shaped focal spot for illumination and a line of CMOS imaging sensor pixels for detection, resulting in enhancement of pixel resolving power in one direction.[89] Their imaging platform can provide multiple fluorescence collection channels with high resolution and high throughput.

Scanning-based optofluidic imaging systems, when coupled with high throughput hydrodynamic focusing systems can potentially lead to the development of high-speed imaging-based flow cytometery on a chip level and enable large scale analysis.[90–92] Optofluidic imaging systems also enable integration of other lab-on-a-chip functionalities, for example, cell/micro-organism filtering, sorting and harvesting. However, using microfluidics as a means for sample scanning does have the following limitations. First, the microfluidic motion of translating biological samples is subjected to Brownian fluctuation, which can cause blurring and distortion of the image. For some samples, such as blood cells or micro-organisms, with a size of tens of microns, Brownian motion may not have much an effect. However, for smaller entities, such as bacteria and virus particles, which are usually less than one micron, Brownian motion becomes significant and results in sample fluctuation. Second, we have to make sure the microfluidic channel is blockage free and clean. Although some bio-assay and surface chemistry methods described earlier may help to promote lubrication, pre-filtering may be required to load samples to the

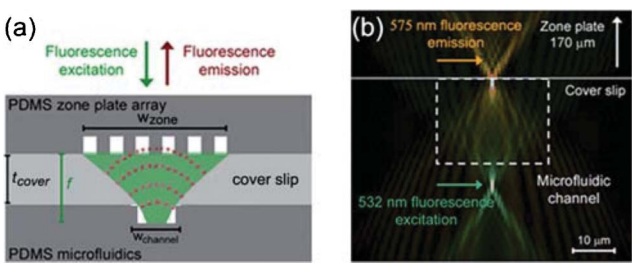

Fig. 8 Light excitation and collection by the FZP microfluidic device (a) schematic illustration; (b) numerical simulation of light intensity distribution. Images are acquired from ref. 88.

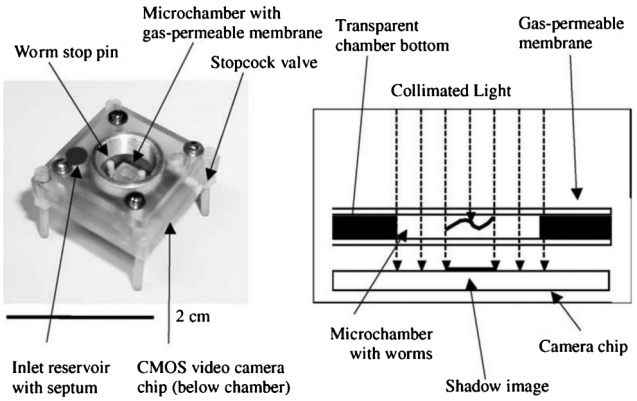

Fig. 9 Photograph and schematic of the microfluidic shadow imaging system. Image is acquired from ref. 93.

microfluidic device. Lastly and probably the fundamental limitation of scanning-based optofluidic systems: since the biological samples have to be suspended in a liquid medium, scanning-based optofluidic imaging is generally not applicable for attached or confluent samples, for example in neural or tissue engineering applications. In addition, the biological samples have to maintain a constant orientation and shape during the microfluidic translation for good imaging formulation. This greatly hinders the possibility for dynamics or time-lapse studies, like cell-division, micro-organism-movement tracking and sperm mortality studies. This motivates the development of other types of compact imaging systems, which will be discussed in the next section.

Other compact imaging systems

A natural way to build compact imaging systems is to utilize shadow imaging, where the sample is put on an imaging sensor and its shadow is observed directly. In the microfluidic device, the microchannel is directly stuck on top of the imaging sensor.[93–96] An example is shown in Fig. 9, developed by Lange *et al.*,[93] where the nematode *C. elegans* in the microfluidic channel can be imaged directly by the sensor. Another example is the lensless, ultra wide-field cell monitoring array platform based on shadow imaging (LUCAS), developed by Ozcan *et al.*[94] Their system was able to monitor various different cell types, *e.g.*, blood cells, NIH-3T3 fibroblasts, *etc.* LUCAS and other shadow

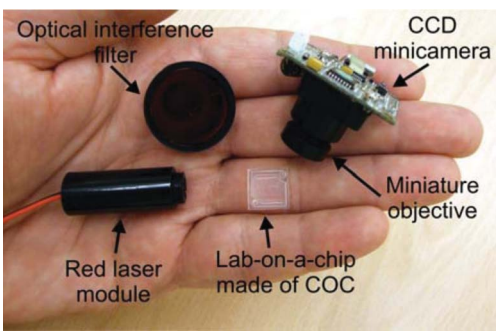

Fig. 10 Optical components of the compact fluorescence detection instrumentation. Image is acquired from ref. 99.

Table 1 Optical imaging methods in microfluidics

Methods	Cost	Size	Resolution	Field-of-view
Conventional Microscope	High	Large	High	Small
Optical coherence tomography (OCT)	High	Large	Low, usually used to detect flow speed	Large
Digital in-line holography	Low	Compact	Moderate	Large
Optofluidic microscopy (OFM)	Low	Compact	Moderate	Moderate, depends on applications
Shadow imaging	Low	Compact	Low	Large
Subpixel perspective sweeping microscopy (SPSM)	Low	Compact	Moderate	Large
Compact lens-imaging systems	Low	Moderate	Moderate	Small

imaging techniques[95,96] showed potential applications in point-of-care cell counting for HIV monitoring. Results of counting $CD4^+$ T-lymphocytes from blood with bright-field and fluorescence imaging were shown in ref. 95. Note that LUCAS was later combined with digital in-line holography scheme to obtain better imaging capabilities as discussed previously.

The imaging system based on direct shadow imaging is simple and robust. However, the image resolution is usually not satisfactory. In this case, the resolution is limited by the pixel size of the sensor and the distance between the sample and the sensor. On the one hand, a CMOS sensor currently can have a pixel size down to 1.6 microns and thus the best resolution that can be achieved by shadow imaging is 3.2 microns by the Nyquist sampling theorem. Smaller pixel sizes might be possible in the future with the trade-off of less light sensitivity. On the other hand, the distance between the sample and the sensor is determined by the height of the microchannel and the nature of the microfluidic flow. Furthermore, shadow imaging cannot be used for efficient fluorescence imaging because of low excitation efficiency and poor resolution. Because of these limitations, direct shadow imaging can only be used in applications where image resolution is not important.

Interestingly, it is possible to achieve better resolution using shadow imaging if combing multiple shadow images. Zheng *et al.* developed an on-chip lensless imaging technique termed subpixel perspective sweeping microscopy (SPSM).[97] In their setup, the illumination was tilted/shifted incrementally and the shadow images of the sample were captured while moving across the sensor pixels. These sub-pixel shifted low-resolution images can then be used to reconstruct a high-resolution image by using a pixel-super-resolution algorithm similar to in ref. 84. It is worth noting that this technique can achieve higher resolution ($\sim$660 nm in ref. 84) and can be very compact. However, the disadvantage is that the imaging speed is slow because of the requirement to acquire a series of shadow images before reconstructing the high-resolution image. Thus it is perfect for cell culture growth observations that happen over a large time scale,[97] while not suitable for observing fast dynamics of a sample.

To overcome the limitation of SPSM, Lee *et al.* developed the sub-pixel motion microscopy (SPMM),[98] where a similar idea to SROFM was used. Instead of utilizing microfluidic flow to move the sample as in SROFM, SPMM relies on the autonomous motion of the sample which is alive. Using the pixel-super-resolution algorithm, multiple shadow images were combined to reconstruct a high-resolution image. Both SPSM and SPMM can be used to construct the ePetri dish platform for biological studies.

The other way to achieve a compact imaging device is to reduce the size and get rid of unimportant attachments of a lens imaging system. For example, Walczak introduced a miniaturized instrumentation for fluorescence detection,[99] as shown in Fig. 10. In their imaging system, all components are miniaturized and the total size can be greatly reduced compared with conventional microscope. Their system has been used as a real-time PCR analyzer for demonstration.

The principle of compact lens imaging systems is the same as conventional microscope. And it's obvious that there is a trade-off between the size and the image quality. In the example shown in Fig. 10, the miniature objective cannot have the same quality as a microscope objective in terms of numerical aperture and aberration correction. Thus it is used for fluorescence detection instead of imaging the details of the sample. If a larger size is allowed, microscope objectives can be used to build compact imaging systems, as presented in ref. 100 and 101. The acquired image will have similar quality as those acquired by conventional microscope with the same objective lens. These systems can be readily used with microfluidic devices.

Conclusions

In this review, we summarize and discuss various optical imaging techniques used in microfluidics, including bulky imaging techniques, digital in-line holography, scanning-based imaging techniques, and other compact imaging systems. Comparison of some important imaging methods in terms of cost, size, imaging resolution and field-of-view is summarized in Table 1. Note that all imaging methods have their pros and cons and their usage should depend on the specific application.

Optical imaging is an intuitive way to observe the samples in microfluidic devices and contains rich information. Conventional bulky imaging techniques still dominate in microfluidic applications. However, we believe that the on-chip imaging methods and systems are promising and should provide a compact and low-cost solution, especially in the case of field applications. And we expect to see more research efforts in this area.

References

1 G. M. Whitesides, *Nature*, 2006, **442**, 368–373.
2 D. Erickson and D. Li, *Anal. Chim. Acta*, 2004, **507**, 11–26.
3 D. Psaltis, S. R. Quake and C. Yang, *Nature*, 2006, **442**, 381–386.
4 X. Fan and I. M. White, *Nat. Photonics*, 2011, **5**, 591–597.
5 H. C. Hunt and J. S. Wilkinson, *Microfluid. Nanofluid.*, 2008, **4**, 53–79.
6 V. R. Horowitz, D. D. Awschalom and S. Pennathur, *Lab Chip*, 2008, **8**, 1856–1863.

7 B. Kuswandi, J. Huskens and W. Verboom, *Anal. Chim. Acta*, 2007, **601**, 141–155.
8 K. B. Mogensen, H. Klank and J. P. Kutter, *Electrophoresis*, 2004, **25**, 3498–3512.
9 C. Yi, Q. Zhang, C. W. Li, J. Yang, J. Zhao and M. Yang, *Anal. Bioanal. Chem.*, 2006, **384**, 1259–1268.
10 A. Q. Liu, H. J. Huang, L. K. Chin, Y. F. Yu and X. C. Li, *Anal. Bioanal. Chem.*, 2008, **391**, 2443–2452.
11 J. Wu and M. Gu, *J. Biomed. Opt.*, 2011, **16**, 080901.
12 U. A. Gurkan, S. Moon, H. Geckil, F. Xu, S. Wang, T. J. Lu and U. Demirci, *Biotechnol. J.*, 2011, **6**, 138–149.
13 G. Zheng, *J. Biophotonics*, 2012, **5**, 639–649.
14 L. Huang, S. J. Maerkl and O. J. F. Martin, *Opt. Express*, 2009, **17**, 6018–6024.
15 M. J. Levene, J. Korlach, S. W. Turner, M. Foquet, H. G. Craighead and W. W. Webb, *Science*, 2003, **299**, 682–686.
16 A. H. J. Yang, S. D. Moore, B. S. Schmidt, M. Klug, M. Lipson and D. Erickson, *Nature*, 2008, **457**, 71–75.
17 W. J. A. Koopmans, T. Schmidt and J. van Noort, *ChemPhysChem*, 2008, **9**, 2002–2009.
18 S. Hu, X. Ren, M. Bachman, C. E. Sims, G. P. Li and N. Allbritton, *Electrophoresis*, 2003, **24**, 3679–3688.
19 E. Vasdekis and G. P. J. Laporte, *Int. J. Mol. Sci.*, 2011, **12**, 5135–5156.
20 P. C. H. Li, L. de Camprieu, J. Cai and M. Sangar, *Lab Chip*, 2004, **4**, 174–180.
21 J. W. Kim, A. S. Utada, A. Fernández-Nieves, Z. Hu and D. A. Weitz, *Angew. Chem.*, 2007, **119**, 1851–1854.
22 J. P. Shelby, J. White, K. Ganesan, P. K. Rathod and D. T. Chiu, *Proc. Natl. Acad. Sci. U. S. A.*, 2003, **100**, 14618–14622.
23 Z. Yang, S. Matsumoto, H. Goto, M. Matsumoto and R. Maeda, *Sens. Actuators, A*, 2001, **93**, 266–272.
24 Y. Zeng, L. Jiang, W. Zheng, D. Li, S. Yao and J. Y. Qu, *Opt. Lett.*, 2011, **36**, 2236–2238.
25 B. G. Chung, L. A. Flanagan, S. W. Rhee and P. H. Schwartz, *Lab Chip*, 2005, **5**, 401–406.
26 R. Yokokawa, S. Takeuchi, T. Kon, M. Nishiura, K. Sutoh and H. Fujita, *Nano Lett.*, 2004, **4**, 2265–2270.
27 C. Simonnet and A. Groisman, *Appl. Phys. Lett.*, 2005, **87**, 114104.
28 C. W. Hollars, J. Puls, O. Bakajin, B. Olsan, C. E. Talley, S. M. Lane and T. Huser, *Anal. Bioanal. Chem.*, 2006, **385**, 1384–1388.
29 L. Cai, N. Friedman and X. S. Xie, *Nature*, 2006, **440**, 358–362.
30 Y. Luo, W. Sun, C. Liu, G. Wang and N. Fang, *Anal. Chem.*, 2011, **83**, 5073–5077.
31 A. Graneli, C. C. Yeykal, T. K. Prasad and E. C. Greene, *Langmuir*, 2006, **22**, 292–299.
32 D. Huang, E. A. Swanson, C. P. Lin, J. S. Schuman, W. G. Stinson, W. Chang, M. R. Hee, T. Flotte, K. Gregory, C. A. Puliafito and J. G. Fujimoto, *Science*, 1991, **254**, 1178–1181.
33 M. E. Brezinski, *Optical Coherence Tomography: Principles and Applications*, Academic Press, 2006.
34 Y. Zhao, Z. Chen, C. Saxer, S. Xiang and J. F. de Boer, *Opt. Lett.*, 2000, **25**, 114–116.
35 L. Wang, W. Xu, M. Bachman, G. P. Li and Z. Chen, *Appl. Phys. Lett.*, 2004, **85**, 1855–1857.
36 C. Xi, D. L. Marks, D. S. Parikh, L. Raskin and S. A. Boppart, *Proc. Natl. Acad. Sci. U. S. A.*, 2004, **101**, 7516–7521.
37 J. Kim, J. Oh, T. E. Milner and J. S. Nelson, *Nanotechnology*, 2007, **18**, 035504.
38 Y. C. Ahn, W. Jung and Z. Chen, *Lab Chip*, 2008, **8**, 125–133.
39 S. Cito, Y. C. Ahn, J. Pallares, R. M. Duarte, Z. Chen, M. Madou and I. Katakis, *Microfluidics and Nanofluidics*, 2012, DOI: 10.1007/s10404-012-0950-6.
40 M. A. Choma, M. V. Sarunic, C. Yang and J. A. Izatt, *Opt. Express*, 2003, **11**, 2183–2189.
41 G. Popescu, *Methods Cell Biol.*, 2008, **90**, 87–115.
42 N. Lue, G. Popescu, T. Ikeda, R. R. Dasari, K. Badizadegan and M. S. Feld, *Opt. Lett.*, 2006, **31**, 2759–2761.
43 J. Atencia and D. J. Beebe, *Nature*, 2005, **437**, 648–655.
44 J. Wu, Z. Yaqoob, X. Heng, L. M. Lee, X. Cui and C. Yang, *Appl. Phys. Lett.*, 2007, **90**, 151123.
45 D. Paganin and K. A. Nugent, *Phys. Rev. Lett.*, 1998, **80**, 2586–2589.
46 S. S. Gorthi and E. Schonbrun, *Opt. Lett.*, 2012, **37**, 707–709.
47 H. Hufnagel, A. Huebner, C. Gulch, K. Guse, C. Abell and F. Hollfelder, *Lab Chip*, 2009, **9**, 1576–1582.
48 S. Choi and J. K. Park, *Small*, 2010, **6**, 1306–1310.
49 M. Abkarian, M. Faivre and H. A. Stone, *Proc. Natl. Acad. Sci. U. S. A.*, 2006, **103**, 538–542.
50 W. Song and D. Psaltis, *Biomicrofluidics*, 2011, **5**, 044110.
51 D. Gabor, *Nature*, 1948, **161**, 777–778.
52 L. Repetto, E. Piano and C. Pontiggia, *Opt. Lett.*, 2004, **29**, 1132–1134.
53 W. Xu, M. Jericho, I. Meinertzhagen and H. Kreuzer, *Proc. Natl. Acad. Sci. U. S. A.*, 2001, **98**, 11301–11305.
54 J. Garcia-Sucerquia, W. Xu, S. K. Jericho, P. Klages, M. H. Jericho and H. J. Kreuzer, *Appl. Opt.*, 2006, **45**, 836–850.
55 O. Mudanyali, D. Tseng, C. Oh, S. O. Isikman, I. Sencan, W. Bishara, C. Oztoprak, S. Seo, B. Khademhosseini and A. Ozcan, *Lab Chip*, 2010, **10**, 1417–1428.
56 J. Garcia-Sucerquia, W. Xu, M. H. Jericho and H. J. Kreuzer, *Opt. Lett.*, 2006, **31**, 1211–1213.
57 D. Tseng, O. Mudanyali, C. Oztoprak, S. O. Isikman, I. Sencan, O. Yaglidere and A. Ozcan, *Lab Chip*, 2010, **10**, 1787–1792.
58 J. B. Develis, J. G. B. Parrent and B. J. Thompson, *J. Opt. Soc. Am.*, 1966, **56**, 423–427.
59 U. Schnars and W. Juptner, *Digital holography: digital hologram recording, numerical reconstruction, and related techniques*, Springer, 2005.
60 J. R. Fienup, *Opt. Lett.*, 1978, **3**, 27–29.
61 J. R. Fienup, *J. Opt. Soc. Am. A*, 1987, **4**, 118–123.
62 G. Liu and P. Scott, *J. Opt. Soc. Am. A*, 1987, **4**, 159–165.
63 G. Koren, F. Polack and D. Joyeux, *J. Opt. Soc. Am. A*, 1993, **10**, 423–433.
64 A. Jesacher, W. Harm, S. Bernet and M. Ritsch-Marte, *Opt. Express*, 2012, **20**, 5470–5480.
65 J. J. Barton, *Phys. Rev. Lett.*, 1991, **67**, 3106–3109.
66 Y. Takaki, H. Kawai and H. Ohzu, *Appl. Opt.*, 1999, **38**, 4990–4996.
67 I. Yamaguchi and T. Zhang, *Opt. Lett.*, 1997, **16**, 1268–1269.
68 J. Garcia-Sucerquia, W. Xu, S. Jericho, M. Jericho and H. J. Kreuzer, *Optik*, 2008, **119**, 419–423.
69 W. Bishara, H. Zhu and A. Ozcan, *Opt. Express*, 2010, **18**, 27499–27510.
70 J. Rodenburg, A. Hurst and A. Cullis, *Ultramicroscopy*, 2007, **107**, 227–231.
71 F. Zhang, G. Pedrini and W. Osten, *Phys. Rev. A: At., Mol., Opt. Phys.*, 2007, **75**, 043805.
72 J. R. Fienup and C. C. Wackerman, *J. Opt. Soc. Am. A*, 1986, **3**, 1897–1907.
73 D. Shin, M. Daneshpanah, A. Anand and B. Javidi, *Opt. Lett.*, 2010, **35**, 4066–4068.
74 A. F. Coskun, T. W. Su and A. Ozcan, *Lab Chip*, 2010, **10**, 824–827.
75 M. Shotton, *J. Cell Sci.*, 1989, **94**, 175–206.
76 M. Minsky, *Microscopy apparatus*, US Patent Number 3,013,467, 1961.
77 S. Kwon and L. P. Lee, *Opt. Lett.*, 2004, **29**, 706–708.
78 D. L. Dickensheets and G. S. Kino, *Opt. Lett.*, 1996, **21**, 764–766.
79 E. A. Ash and G. Nicholls, *Nature*, 1972, **237**, 510–512.
80 U. Dürig, D. Pohl and F. Rohner, *J. Appl. Phys.*, 1986, **59**, 3318–3327.
81 X. Heng, D. Erickson, L. R. Baugh, Z. Yaqoob, P. W. Sternberg, D. Psaltis and C. Yang, *Lab Chip*, 2006, **6**, 1274–1276.
82 X. Cui, L. M. Lee, X. Heng, W. Zhong, P. W. Sternberg, D. Psaltis and C. Yang, *Proc. Natl. Acad. Sci. U. S. A.*, 2008, **105**, 10670–10675.
83 L. M. Lee, X. Cui and C. Yang, *Biomed. Microdevices*, 2009, **11**, 951–958.
84 G. Zheng, S. A. Lee, S. Yang and C. Yang, *Lab Chip*, 2010, **10**, 3125–3129.
85 S. A. Lee, R. Leitao, G. Zheng, S. Yang, A. Rodriguez and C. Yang, *PLoS One*, 2011, **6**, e26127.
86 J. Wu, X. Cui, L. M. Lee and C. Yang, *Opt. Express*, 2008, **16**, 15595–15602.
87 S. Pang, C. Han, L. M. Lee and C. Yang, *Lab Chip*, 2011, **11**, 3698–3702.
88 E. Schonbrun, A. R. Abate, P. E. Steinvurzel, D. A. Weitz and K. B. Crozier, *Lab Chip*, 2010, **10**, 852–856.
89 X. Heng, F. Hsiung, A. Sadri and P. Patt, *Anal. Chem.*, 2011, **83**, 1587–1593.

90 S. C. Hur, H. T. K. Tse and D. Di Carlo, *Lab Chip*, 2010, **10**, 274–280.
91 N. Sundararajan, M. S. Pio, L. P. Lee and A. A. Berlin, *J. Microelectromech. Syst., 2004, 13*, **559**, -567.
92 M. Oheim, *Br. J. Pharmacol.*, 2007, **152**, 1–4.
93 D. Lange, C. W. Storment, C. A. Conley and G. T. A. Kovacs, *Sens. Actuators, B*, 2005, **107**, 904–914.
94 A. Ozcan and U. Demirci, *Lab Chip*, 2008, **8**, 98–106.
95 S. J. Moon, H. O. Keles, A. Ozcan, A. Khademhosseini, E. Haeggstrom, D. Kuritzkes and U. Demirci, *Biosens. Bioelectron.*, 2009, **24**, 3208–3214.
96 W. G. Lee, Y. G. Kim, B. G. Chung and U. Demirci, *Adv. Drug Delivery Rev.*, 2010, **62**, 449–457.
97 G. Zheng, S. A. Lee, Y. Antebi, M. B. Elowitz and C. Yang, *Proc. Natl. Acad. Sci. U. S. A.*, 2011, **108**, 16889–16894.
98 S. A. Lee, G. Zheng, N. Mukherjee and C. Yang, *Lab Chip*, 2012, **12**, 2385–2390.
99 R. Walczak, *BioChip J.*, 2011, **5**, 271–279.
100 D. N. Breslauer, R. N. Maamari, N. A. Switz, W. A. Lam and D. A. Fletcher, *PLoS One*, 2009, **4**, e6320.
101 D. Shin, M. C. Pierce, A. M. Gillenwater, M. D. Williams and R. R. Richards-Kortum, *PLoS One*, 2010, **5**, e11218.